Talanta 122 (2014) 16–22

Contents lists available at ScienceDirect

Talanta

journal homepage: www.elsevier.com/locate/talanta

A novel urea-linked dipodal naphthalene-based fluorescent sensor for Hg(II) and its application in live cell imaging

Kundan Tayade [a,b], Banashree Bondhopadhyay [d], Anupam Basu [d], G. Krishna Chaitanya [c], Suban K. Sahoo [e], Narinder Singh [f], Sanjay Attarde [b,*], Anil Kuwar [a,**]

[a] School of Chemical Sciences, North Maharashtra University, Jalgaon-425001, Maharashtra, India
[b] School of Environmental and Earth Sciences, North Maharashtra University, Jalgaon-425001, Maharashtra, India
[c] School of Chemical Sciences, Swami Ramanand Teerth Marathawada University, Nanded, Maharashtra, India
[d] Molecular Biology and Human Genetics Laboratory, Department of Zoology, The University of Burdwan, Burdwan, West Bengal, India
[e] Department of Applied Chemistry, SV National Institute Technology, Surat-395007, Gujrat, India
[f] Department of Chemistry, Indian Institute Technology, Ropar, Rupnagar, Punjab, India

ARTICLE INFO

Article history:
Received 3 November 2013
Received in revised form
28 December 2013
Accepted 30 December 2013
Available online 21 January 2014

Keywords:
Fluorescent sensor
Hg^{2+}
Turn-off
Cellular imaging
Real sample analysis
DFT

ABSTRACT

A novel cell-permeable urea-linked dipodal naphthalene-based fluorescent receptor **1** (1,1'-(1,5,5-trimethyl-3-oxocyclohexane-1,2-diyl)bis(3-(naphthalen-2-yl)urea) was designed and synthesized. The cation recognition ability of **1** was evaluated with a library of metal ions in DMSO/H_2O (9:1, v/v). The receptor showed a selective chromogenic and fluorescent turn-off response towards Hg^{2+} among the surveyed metal ions. The developed sensor was successfully applied to image intracellular Hg^{2+} in living cells and also for the determination of Hg^{2+} content in real water samples. Moreover, the DFT calculations were performed to complement the experimental evidences.

1. Introduction

Topologically interesting amide and urea/thiourea based fluorescent probes mostly appended to organic scaffolds leading to the formulation of anion coordination chemistry [1]. The literature survey reveals that these receptors are on the verge of getting transformed towards judicial use in cation recognition [2,3], but further exploration is required for the development of more selective, efficient and cost-effective receptors. Also, there are some noteworthy contests in the designing of Hg^{2+} sensors particularly on desulfurization-based, however, under the sulfur-rich environment, the sensing process suffered particularly from the excess requirement of Hg^{2+} or elevated temperatures [4,5].

It is well known that far and wide distribution of mercury and its derivatives are enormously poisonous, and enter the environment through a variety of natural and anthropogenic sources producing prevalent anxiety due to their severe effect to the environment and flora and fauna [6]. The accretion of mercury ions in human body can induce various diseases, such as prenatal brain damage, serious cognitive, motion disorders and minamata disease [7–9]. A key source of human revelation is Hg^{2+} in contaminated natural water, and therefore there is a need of simple, convenient, rapid, cost-effective and selective method for the sensing of Hg^{2+} in aqueous media. For these reasons, the development of well-organized fluorogenic and chromogenic receptors giving a worthy response towards the mercury ion has fetched a great attention due to the advantages of simplicity, sensitivity, specificity and minimization of sophisticated instrumentation compared to other analytical methods, such as electro-analytical techniques and atomic absorption spectrometry [10,11].

In the present study, we have designed and synthesized a flexible dipodal receptor **1** for the selective recognition of Hg^{2+} in DMSO/H_2O (9:1, v/v) by using the chromogenic and fluorogenic turn-off modes. The analytical applications of **1** were tested for the detection of Hg^{2+} in living cells and real water samples. Also, the experimental evidences were complemented with the theoretical (DFT) results.

2. Experimental

2.1. Chemicals and instrumentation

All the solvents, reagents and metal salts were purchased from Sigma-Aldrich Ltd and were used as received unless otherwise

* Corresponding author.
** Corresponding author. Tel.: +91 257 2257432; fax: +91 257 2257403.
E-mail address: kuwaras@gmail.com (A. Kuwar).

0039-9140/$ - see front matter © 2014 Elsevier B.V. All rights reserved.
http://dx.doi.org/10.1016/j.talanta.2013.12.067

mentioned. All absorbance and fluorescence spectra were recorded on a Shimadzu UV–Visible 2400 spectrophotometer and HORIBA JOBIN YVON Fluoromax-4 Spectrofluorometer, respectively. The ^{1}H and ^{13}C NMR spectra were recorded on a Bruker AV-400 and 100 MHz spectrometer. The infrared spectra were recorded on a Perkin Elmer Spectrum spectrometer, using Nujol Mull. Mass spectra of receptor **1** and **1**.Hg^{2+} complex were obtained on Bruker Ultraflex II MALDI/TOF spectrometer. Thermal analysis study was carried out on Perkin Elmer DSC 400 and Perkin Elmer TGA 400.

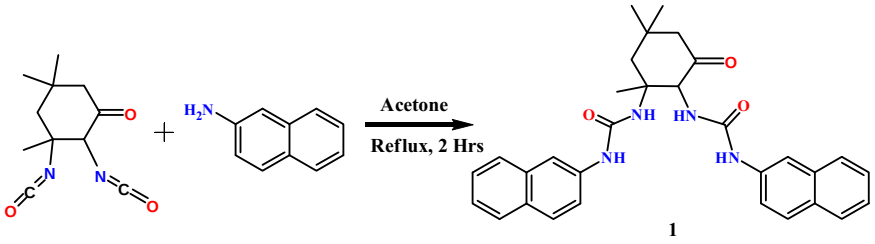

Scheme 1. Synthesis of receptor **1**.

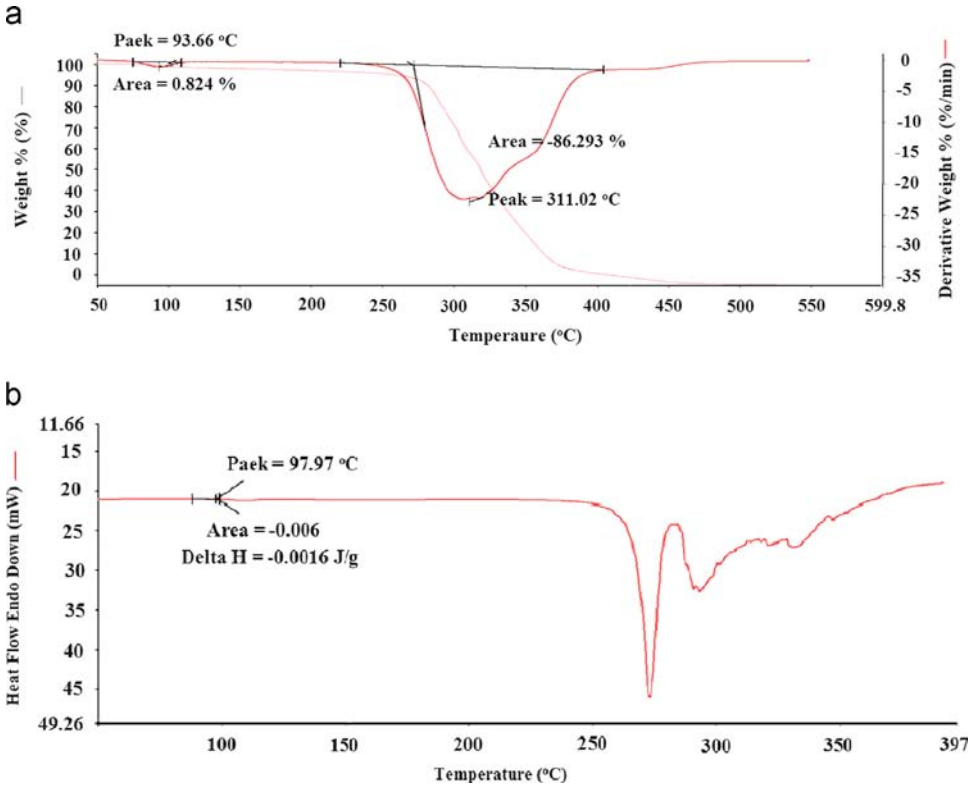

Fig. 1. (a) TGA (at the heating rate of 10 °C min^{-1}) and (b) DSC graphs of receptor **1**.

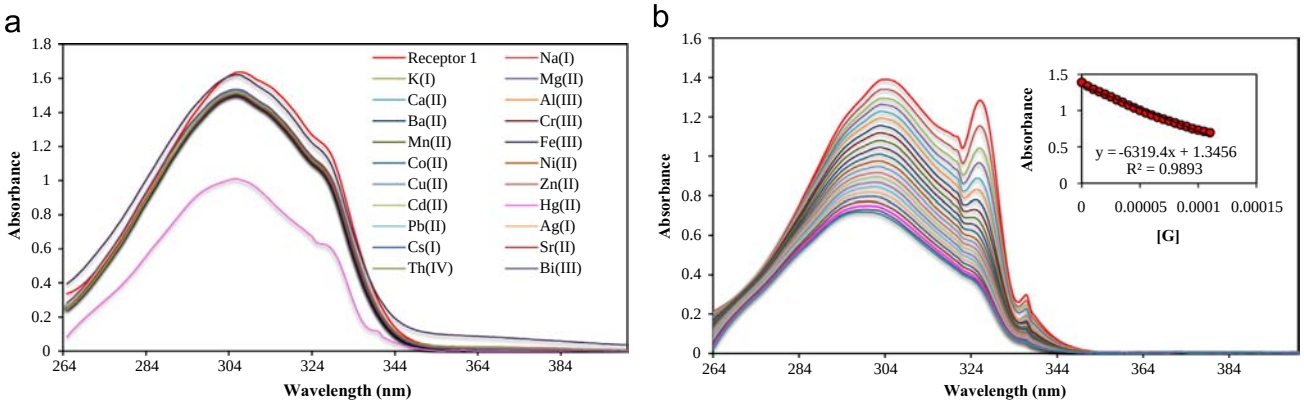

Fig. 2. (a) Absorption spectra of receptor **1** (1×10^{-4} M) upon addition of various metal salts. (b) Absorption titration of receptor **1** (1×10^{-4} M) upon addition of increasing amounts of Hg^{2+} (1×10^{-3} M) in DMSO/H_2O (9:1, v/v). Inset showing the graph between [*G*] vs. absorbance at 307 nm; where [*G*] is [Hg^{2+}].

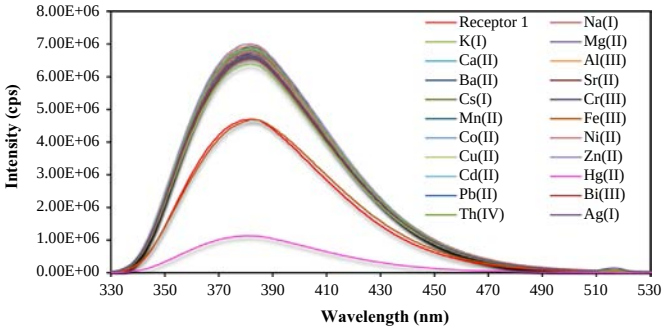

Fig. 3. Fluorescence spectra (λ_{exc}=307 nm and λ_{em}=382 nm) of receptor **1** (1×10^{-4} M) in the absence and presence of different metal ions (1×10^{-3} M, 100 μL) in DMSO/H_2O (9:1, v/v).

2.2. Synthesis of receptor 1

The solution of 2,4-diisocyanato-1-methylbenzene (0.22 g, 1 mmol) in acetone (25 mL) was mixed with the solution of naphthalen-2-amine (0.28 g, 2 mmol) in acetone (25 mL) at room temperature. The reaction mixture was stirred and refluxed for 2 h. Then, the mixture was cooled and the pinkish-white colored precipitate was filtered followed by washed with cold ethanol and dried under vacuum. Yield: 84%; FTIR (Nujol mull, cm^{-1}): 3342, 3051, 2924, 2854, 1637, 1574, 1463, 1377, 1343, 1245,1136, 778,722, 678, 559; ^{1}H NMR (400 MHz, δ, ppm, DMSO-d_6): 0.96 (s, 3*H*, –CH_3), 1.08 (s, 6*H*, 2-CH_3), 1.73 (s, 2*H*, –CH_2), 3.00 (s, 2*H*, –CH_2), 3.86 (s, 1*H*, –CH–), 6.54 (s, 1*H*, NH–), 6.75 (s, 1*H*, –NH), 7.51–8.08 (m, 14*H*, Ar-H), 8.4 (s, 1*H*, –NH), 8.55 (s, 1*H*, –NH–); ^{13}C NMR (100 MHz, δ, ppm, DMSO-d_6): 23.7, 28.0, 32.1, 36.6, 40.5, 43.1, 47.5, 53.5, 116.4,

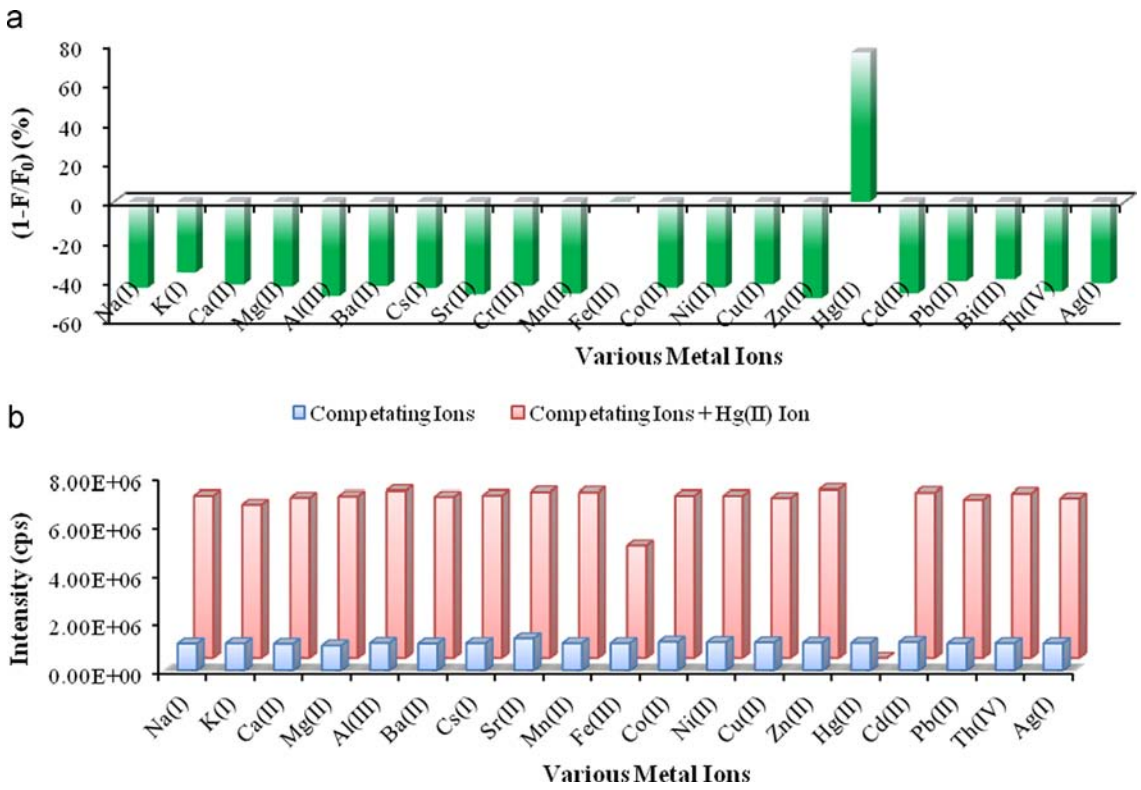

Fig. 4. (a) Fluorescence quenching efficiency of receptor **1** (2000 μL, 1×10^{-4} M) in the presence of various metal ions (100 μL, 1×10^{-3} M). (b) Plot of interference of various surveyed metal ions (400 μL, 2 equiv.) in Hg^{2+} ion (100 μL, 0.5 equiv.) determination by receptor **1** (2000 μL).

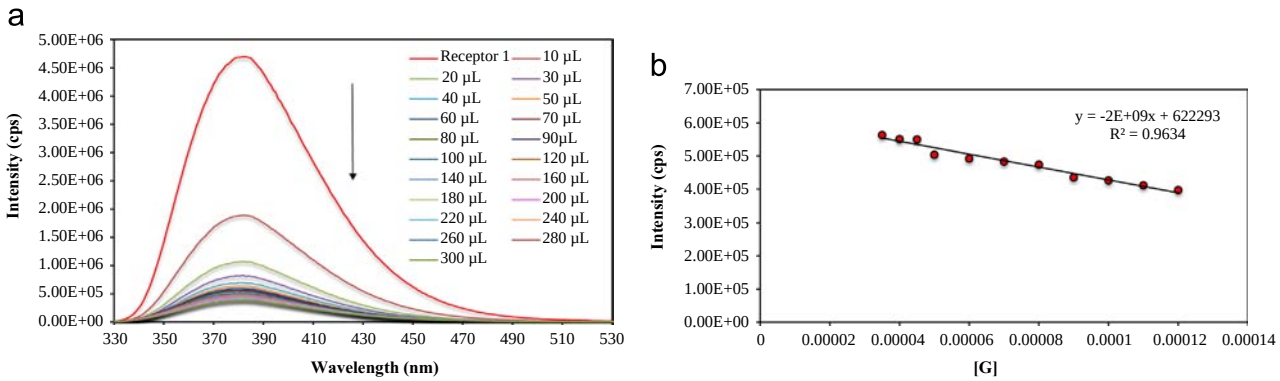

Fig. 5. (a) Fluorescence titration of receptor **1** (1×10^{-4} M) with varying concentrations of Hg^{2+} (1×10^{-3} M) in DMSO/H_2O (9:1, v/v). (b) Normalized plot for determination of detection limit and limit of quantification of receptor **1** which responds to Hg^{2+} ion in the micromolar level; where [*G*] is [Hg^{2+}].

116.5, 121.6, 122.2, 122.3, 125.8, 128.9, 134.1, 135.6, 135.7, 155.3, 156.2, 209.3; MS (ESI): *m*/*z* (%): 510 (32%), 509 (100%).

2.3. UV–visible and fluorescence spectral measurements

The metal ions Na^+, K^+, Ca^{2+}, Mg^{2+}, Al^{3+}, Ba^{2+}, Ce^{3+}, Fe^{3+}, Co^{2+}, Ni^{2+}, Cu^{2+}, Zn^{2+}, Hg^{2+}, Pb^{2+}, Cd^{2+}, Th^{4+} and Ag^+ were added as their nitrate salts where as Sr^{2+} and Mn^{2+} were added as their chloride salts for the different absorption and fluorescence spectroscopic experiments. Stock solutions of metal ions (1×10^{-3} M) and the receptor **1** (1×10^{-4} M) were prepared in DMSO/H_2O (90:10, v/v). These stock solutions were used further for different spectroscopic experiments. The excitation was carried out at 307 nm for receptor **1** with 5 nm emission slit widths in fluorometer. For the absorbance and fluorescence measurements 1 cm width and 3.5 cm height quartz cells were used.

2.4. Cellular imaging study

Cellular imaging experiments were performed according to Lu et al. [12] with modification. Briefly, the human cervical cancer (HeLa) cell was obtained from National Centre for Cell Sciences (NCCS), Pune, India and grown in Dulbecco's Modified Eagle Medium (DMEM) supplemented with 10% Fetal Bovine Serum (FBS), 1% L-glutamine–penicillin–streptomycin and maintained at 37 °C in a humidified atmosphere with 5% CO_2. The cells were seeded on the cover slip in the 35 mm culture dish with a seeding density of 3×10^4 cells per 35 mm dish. After reaching 60% confluence, the cells were serum starved for overnight. Immediately, the cells were washed with serum free media prior to the addition of Hg^{2+}. Cells were treated with 50 μM and 100 μM concentration of Hg^{2+} for 2 h for Hg^{2+} uptake. Cells were washed with 1 × PBS and receptor **1** was added (80 μM) for 2 min at room temperature. The cells were then washed twice with 1 × PBS. The cover slip on which the cells were seeded was mounted on a glass slide and observed under a fluorescence microscope (Leica DM 1000) with an excitation filter at 515 nm.

3. Results and discussion

3.1. Synthesis of receptor 1

The synthesis of receptor **1** is depicted in Scheme 1. Receptor **1** was obtained by refluxing 2,4-diisocyanato-1-methylbenzene with naphthalen-2-amino in acetone. The receptor **1** was obtained with quantitative yield and characterized by several techniques such as IR, ^{1}H-NMR, ^{13}C-NMR and mass spectra (Supporting information, Fig. S1a–d). The spectral investigation gave consistent data for the structure of **1**.

3.2. Thermal analysis of receptor 1

The thermal behavior of receptor **1** was recorded on TGA and DSC as shown in Fig. 1. In TGA, the initial 0.824% decomposition at 93 °C is observed due to the evaporation of water molecules. Owing to the weight loss at lower temperature, these water molecules may be considered as crystal water [13]. The sharp onset decomposition of peak was obtained at 271.3 °C which may be attributed to cleavage of amide linkage. The DSC curve of receptor **1** showed two peaks, which are similar to two decomposition points as seen in the TGA curve. The DSC revealed the sharp endothermic peak at 273.14 °C corresponding to the decomposition of receptor **1** which was in concordance with the results of TGA value.

3.3. Absorption studies of receptor 1

The absorption spectral properties of receptor **1** were studied in the absence and presence of different alkaline and alkaline-earth metal ions (Na^+, K^+, Cs^+, Mg^{2+}, Ca^{2+}, Sr^{2+}, Ba^{2+}), transitions and lanthanides metal ions (Mn^{2+}, Fe^{3+}, Co^{2+}, Ni^{2+}, Cu^{2+}, Zn^{2+}, Hg^{2+}, Pb^{2+}, Cd^{2+}, Th^{4+}, Ag^+) in DMSO/H_2O (9:1, v/v). The free receptor **1** exhibited the characteristic naphthalene unit bands with a strong absorption band at 307 nm and a weak band at 326 nm with $\varepsilon=1.64\times10^5\ M^{-1}\ cm^{-1}$. Interestingly, addition of Hg^{2+} ion resulted in no visual color change of receptors **1** but in absorption spectra, it has shown selective and discriminating quenching in compared to other tested metal ions (Fig. 2a). Further, we investigated the effect of successive increase in the concentration of Hg^{2+} (0–220 μL) on the absorption behavior of receptor **1**, which resulted in the decrease in the absorption maxima both at 307 nm and 326 nm (Fig. 2b).

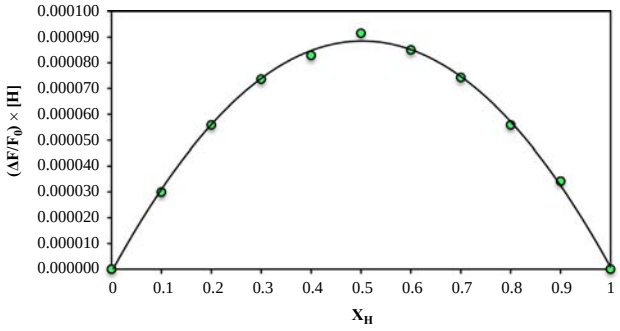

Fig. 6. Job's plot for determining the stoichiometry of receptor **1**.Hg^{2+} ion complexation. Here, $\Delta F=F_0-F$.

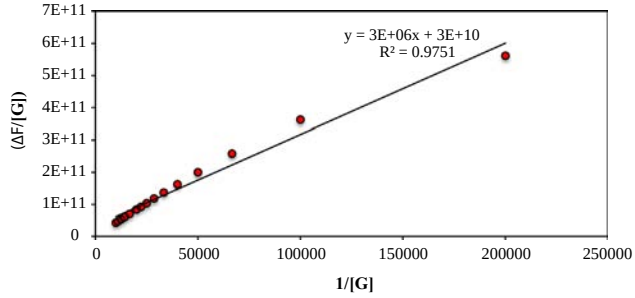

Fig. 7. Plot of ($\Delta F/[G]$) vs. $1/[G]$ for the determination of the affinity constant (K) of receptor **1**.Hg^{2+} ion complexation, $K=3\times10^6\ M^{-1}$; where [G] is [Hg^{2+}].

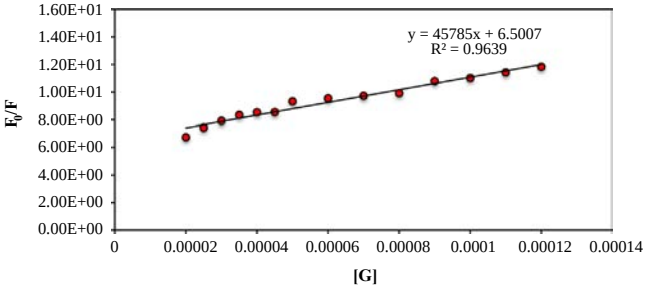

Fig. 8. Stern–Volmer plot for the determination of the affinity constant (K) of receptor **1**.Hg^{2+} ion complexation, $K=3.18\times10^6\ M^{-1}$; where [G] is [Hg^{2+}].

3.4. Fluorescence studies of receptor 1

The fluorescence properties of receptor **1** were next studied in the absence and presence of different metal ions in DMSO/H_2O (90:10, v/v). The receptor **1** exhibited a fluorescence emission at 382 nm, when excited at 307 nm. The fluorescence was selectively and significantly quenched in the presence of Hg^{2+} ions. The quenching response may be due to the enhanced spin–orbit coupling associated with the heavy atom effect of the complexed Hg^{2+} [14]. However, there was no such fluorescence turn-off observed in the emission outline of receptor **1** in the presence of other tested metal ions, which reveals the high selectivity of receptor **1** for Hg^{2+} (Fig. 3).

The competition experiments were conducted in the presence of 0.5 equiv. of Hg^{2+} mixed with excess of other metal ions (2 equiv.). The fluorescence contour of receptor **1** with Hg^{2+} was almost not affected in the co-existence of other interfering metal ions in excess (Fig. 4a and b). These results indicate that the receptor **1** showed a good sensitivity and selectivity towards Hg^{2+} over other competitive metal ions.

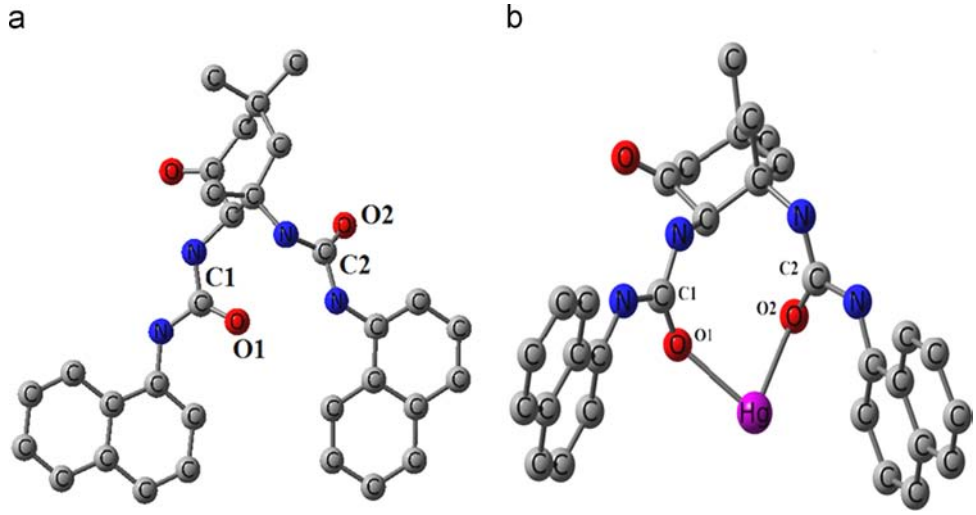

Fig. 9. The DFT optimized geometrical parameters of receptor (a) **1** and (b) **1**.Hg^{2+} complex obtained by using B3LYP/6-31G and B3LYP/LANL2DZ method.

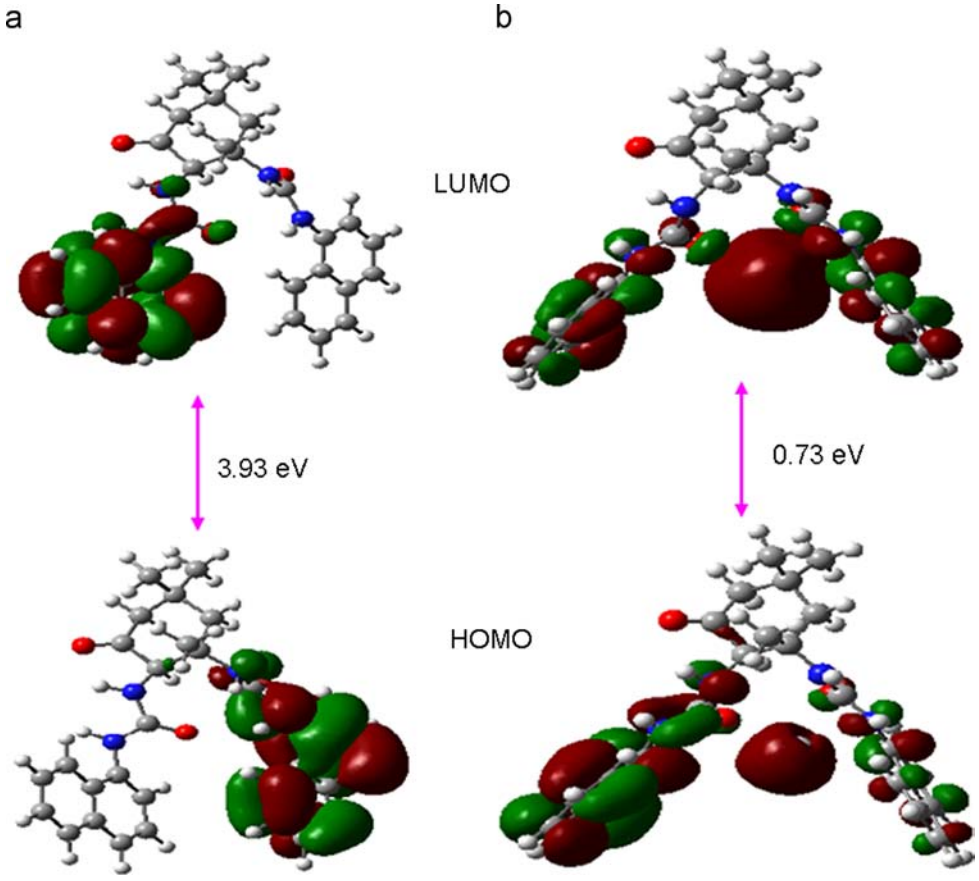

Fig. 10. The HOMO–LUMO gap of (a) receptor **1** and (b) **1**.Hg^{2+} calculated at the B3LYP/6-31G/LanL2DZ level, respectively.

Further, the emission spectroscopy titration of receptor **1** was carried out with the successive addition of Hg^{2+} (Fig. 5a). The fluorescence intensity of receptor **1** with emission peak maximum at 382 nm was gradually quenched by over seven fold with the addition of increasing amount of Hg^{2+}. Unlike other metal ions, the quenching induced by Hg^{2+} ion suggesting that the complexation described above occurred which also has the advantage of ion discrimination. Meantime, Fig. 5b is made to determine the detection limit of receptor **1**, which responds to Hg^{2+} ion linearly in the micromolar level in its concentration range with the detection limit down to 0.23 μM.

3.5. Stoichiometry of complexation

The stoichiometry for the complexation of receptor **1** with Hg^{2+} was studied using Job's continuous variation method [15]. Job's plot obtained from the fluorescence measurements showed the formation of receptor **1**.Hg^{2+} complex in 1:1 stoichiometric ratio (Fig. 6). This data was further confirmed by mass spectroscopy analysis. MALDI/TOF–MS data showed the formation of a 1:1 complex (**1**.Hg^{2+}) ([receptor**1**.Hg^{2+}]$^{+}$·H_2O, MW = 726.20, calcd for $C_{31}H_{32}N_4O_3Hg \cdot H_2O$, 726.19, Fig. S2a, Supporting information). Further, the infrared spectrum of **1**.Hg^{2+} complex inferred that the $\nu_{C=O}$ of the free receptor at 1637 cm^{-1} was shifted to 1641 cm^{-1} on complexation with Hg^{2+} (Fig. S2b, Supporting information).

Table 1
Some calculated physicochemical (bond lengths and angles) and electronic (band gap) parameters of 1 and 1.Hg^{2+} ion at B3LYP/6-31G/LanL2DZ level.

Parameters	**1**	**1**.Hg^{2+}
C1–O1	1.232 Å	1.255 Å
C2–O2	1.229 Å	1.244 Å
Hg–O1	–	2.392 Å
Hg–O2	–	2.536 Å
O1–Hg–O2	–	79.3°
C1–O1–Hg–O2	–	−77.9°
C2–O2–Hg–O1	–	96.4°
HOMO–LUMO band gap	3.39 eV	0.73 eV

The binding constant was calculated by following the method reported by Chen et al. [16] and was found to be 3×10^6 M^{-1} (Fig. 7). Then, the Stern–Volmer methodology was utilized to probe the nature of the quenching process of receptor **1** upon complexation with Hg^{2+} [17]. Stern–Volmer plot is useful method of presenting data on emission quenching, and the dynamic or static quenching processes can be determined. Plotting relative emission intensities (F_0/F) against quencher concentration [Q] for a static process should yield a linear Stern–Volmer plot. Then, the static quenching (affinity) constant K_{sv} can be obtained from the slope of the plotted line using Eq. (1)

$$(F_0/F) = 1 + K_{sv}[Q] \quad (1)$$

The linear behavior of the Stern–Volmer analysis was observed from Fig. 8, which indicates that, the static quenching process and the dynamic quenching is not significant in the case of receptor **1**. Thus, the fluorescence quenching mechanism of receptor **1**.Hg^{2+} complexation was analyzed and proposed to be a static quenching mode in the range of low Hg^{2+} concentration based on the Stern–Volmer plot where the energy and electron-transfer processes cannot be ruled out.

The computational study was conducted by using the density functional theory (DFT) method in an attempt to better understand the nature of receptor **1** and its interaction with Hg^{2+}. The B3LYP function with 6-31G (for O, C, N, H atoms) and LanL2DZ (only for Hg^{2+}) basis sets was employed for the calculations by using Gaussian 09 program [18]. The B3LYP/6-31G optimization of receptor **1** has resulted a three dimensional structure where the two arms are oriented in the different directions to reduce the stress from steric crowding (Fig. 9). It was observed that the oxygen atoms of urea groups constitute the pseudo cavity for the complexation of metal ions. Meanwhile, the **1**.Hg^{2+} complex was optimized by using B3LYP/6-31G and LanL2DZ basis set for Hg^{2+}. On coordination of Hg^{2+}, there is an increase in the stability of the whole system. The band gap between HOMO and LUMO becomes lower for **1**.Hg^{2+} complex as compared to the receptor **1** alone (Fig. 10, Table 1). Further analyses of the HOMO and LUMO diagrams of receptor **1** and **1**.Hg^{2+} reveals that the electron density distribution of **1** was significantly influenced on

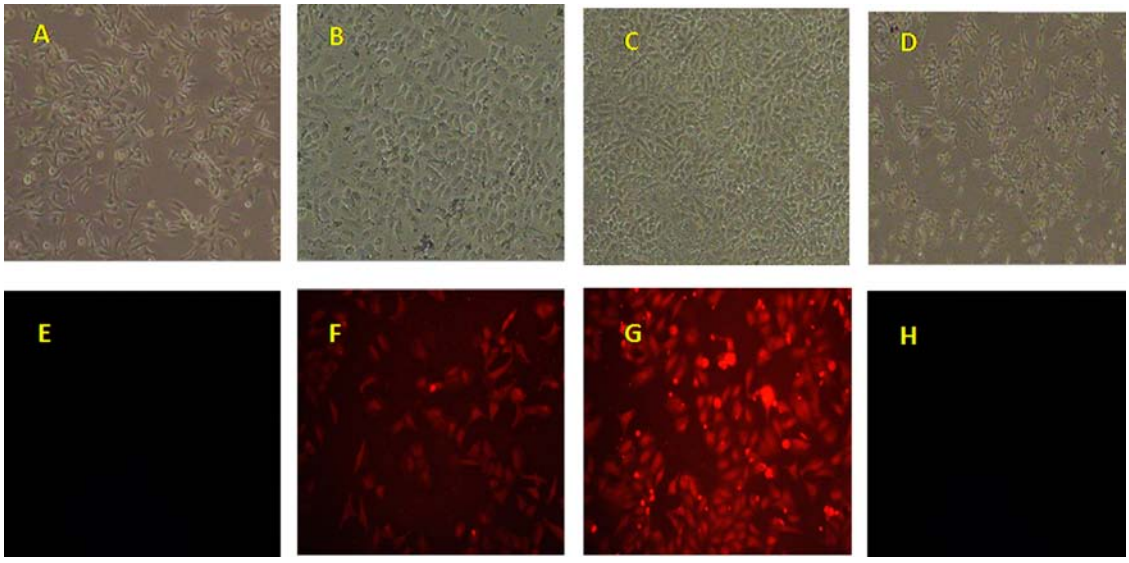

Fig. 11. Fluorescence images of HeLa cells treated with receptor **1** and Hg^{2+}. (A) Phase contrast image of control cells devoid of receptor **1** and Hg (20 ×), (B) phase contrast image of the cells treated with receptor 1, (C) phase contrast image of the cells treated with receptor 1 and Hg^2 (D) phase contrast image of the cells treated with Hg^2 only, (E) fluorescence photo-micrograph of cells neither treated with receptor **1** nor Hg^{2+}, (F) fluorescence photo-micrograph of cells incubated with receptor **1** (80 μM) (20 ×), (G) fluorescence photo-micrograph of cells incubated with receptor **1** (80 μM) and Hg^{2+} (100 μM) (20 ×). (H) Fluorescence photo-micrograph of cells incubated with Hg^{2+} (100 μM) only (20 ×). (All fluorescence images were taken using excitation filter 515 nm).

Table 2
Results of Hg^{2+} sensing in mineral water and well water samples with receptor **1**.

Sample	Amount of Hg^{2+} added ($\mu g\ L^{-1}$)	Amount of Hg^{2+} found ($\mu g\ L^{-1}$)
Mineral water	20	19.95 ± 0.041
	30	30.02 ± 0.050
Well water	20	19.94 ± 0.047
	30	30.04 ± 0.028

complexation with Hg^{2+} due to the possible charge transfer process occurred between the naphthalene units and the Hg^{2+}.

The utility of the sensor in cellular imaging was tested on human cervical cancer cell HeLa. Here, both the receptor **1** and Hg^{2+} were taken up by the cells and the images of the cells were recorded by fluorescence microscopy following excitation at 515 nm (Fig. 11). The receptor **1** has the property of auto-fluorescence, and cells were fluorized when receptor **1** was taken up by the growing cells. When the cells were treated with both Hg^{2+} for 2 h and receptor **1** for 2 min; significant enhancement in fluorescence intensity of the cells was recorded. Thus, it can be said that receptor **1** might be used to visualize the cellular localization.

The practical applicability of the proposed sensing system was also evaluated by determining the Hg^{2+} contents in mineral and well water samples. The water samples were first filtered to remove insoluble substances. All the samples without or with the addition of Hg^{2+} at different concentration levels of 20 $\mu g\ L^{-1}$ and 30 $\mu g\ L^{-1}$ were analyzed by receptor **1** for Hg^{2+} (Table 2). The observed results show that the receptor **1** is able to measure the concentrations of spiked Hg^{2+} with high-quality recovery. This indicates the suitability and practicality of the present receptor **1** for the detection of Hg^{2+} from water samples without any interference from other environmentally relevant competitive metal ions.

4. Conclusion

We report a much easy (noncyclic, one-step synthesis), cost-effective, naphthalene based highly selective fluorescent chemosensor for Hg^{2+} in the presence of other competitive metal ions. The stoichiometry of the complex formation of receptor **1** with Hg^{2+} was determined to be 1:1 using Job's plot and ESI-MS. The detection limit was up to micromolar level. The practical applications in live cells inferred the ability of the receptor **1** to penetrate in Living HeLa cells and detecting intracellular Hg^{2+}. Moreover, the sensor was successfully applied for the determination of Hg^{2+} in different water samples. Therefore, the presence sensing system has great prospective for facile real-time monitoring for Hg^{2+} ion.

Acknowledgement

ASK gratefully acknowledge financial support from the Department of Science and Technology (DST under Fast Track Scheme-SR/FT/CS-160/2011), Government of India, New Delhi. BB and AB express their thanks to DST—SERB for providing the financial support for the Project file No. SR/SO/HS-121/2008.

Appendix A. Supporting information

Supplementary data associated with this article can be found in the online version at http://dx.doi.org/10.1016/j.talanta.2013.12.067.

References

[1] S.O. Kang, R.A. Begum, K.B. James, Angew. Chem. Int. Ed. 45 (2006) 7882–7894.
[2] S.K. Sahoo, M. Baral, J. Photochem. Photobiol., C 10 (2009) 1–20.
[3] (a) B. Gao, W.T. Gong, Q.L. Zhang, J.W. Ye, G.L. Ning, Sens. Actuators, B 162 (2012) 391–395;
(b) M. Mac, T. Uchacz, A. Danel, M.A. Miranda, C. Parisand, U. Pischel, Photochem. Photobiol. Sci. 7 (2008) 633–641.
[4] I.T. Ho, T.L. Lai, R.T. Wu, M.T. Tsai, C.M. Wu, G.H. Lee, W.S. Chung, Analyst 137 (2012) 5770–5776.
[5] L. Chen, L. Yang, H. Li, Y. Gao, D. Deng, Y. Wu, L. Ma, Inorg. Chem. 50 (2011) 10028–10032.
[6] J.F. Zhanga, C.S. Lima, B.R. Choa, J.S. Kim, Talanta 83 (2010) 658–662.
[7] J.S. Lee, M.S. Han, C.A. Mirkn, Angew. Chem. 119 (2007) 4171–4174.
[8] A. Caballero, R. Martınez, V. Lloveras, I. Ratera, J. Vidal-Gancedo, K. Wurst, A. Tarraga, P. Molina, J. Veciana, J. Am. Chem. Soc. 127 (2005) 15666–15667.
[9] S. Bothra, J.N. Solanki, S.K. Sahoo, Sens. Actuators, B 188 (2013) 937–943.
[10] S.K. Sahoo, D. Sharma, R.K. Bera, G. Crisponi, J.F. Callan, Chem. Soc. Rev. 41 (2012) 7195–7227.
[11] (a) J. Wu, E.A. Boyle, Anal. Chim. Acta 367 (1998) 183–191;
(b) O.T. Butler, J.M. Cook, C.F. Harrington, S.J. Hill, J. Rieuwerts, D.L. Miles, J. Anal. At. Spectrom. 21 (2006) 217–243.
[12] H. Lu, L. Xiong, H. Liu, M. Yu, Z. Shen, F. Li, X. You, Org. Biomol. Chem 7 (2009) 2554–2558.
[13] K.N. Patel, N.H. Patel, K.M. Patel, M.N. Patel, Synth. React. Inorg. Met.-Org. Chem. 30 (2000) 921–930.
[14] Q.-Y. Chen, C.-F. Chen, Tetrahedron Lett 46 (2005) 165–168.
[15] P. Job, Ann. Chim. 9 (1928) 113–203.
[16] J. Ding, L. Yuan, L. Gao, J. Chen, J. Lumin. 132 (2012) 1987–1993.
[17] O. Stern, M. Volmer, Phys. J. 20 (1919) 183–188.
[18] M.J. Frisch, et al., Gaussian Inc, Wallingford, CT, 2009.